

Centers of near-infrared luminescence in bismuth-doped TlCl and CsI crystals

V. O. Sokolov,* V. G. Plotnichenko, and E. M. Dianov
*Fiber Optics Research Center of the Russian Academy of Sciences
38 Vavilov Street, Moscow 119333, Russia*

A comparative first-principles study of possible bismuth-related centers in TlCl and CsI crystals is performed and the results of computer modeling are compared with the experimental data of Refs. [1–3]. The calculated spectral properties of the bismuth centers suggest that the IR luminescence observed in TlCl:Bi [1] is most likely caused by $\text{Bi}^+ \cdots \text{V}_{\text{Cl}}^-$ centers (Bi^+ ion in thallium site and a negatively charged chlorine vacancy in the nearest anion site). On the contrary, Bi^+ substitutional ions and Bi_2^+ dimers are most likely responsible for the IR luminescence observed in CsI:Bi [2, 3].

PACS numbers: 22.70.-a, 42.70.Hj, 78.55.-m,

I. INTRODUCTION

New near-IR luminescence, quite different from much-studied Bi^{3+} -related luminescence [4, 5], was discovered in 2001 in bismuth-doped aluminosilicate glass [6]. Then optical amplification at 1.3 μm was demonstrated [7]. Ever since bismuth-doped glasses and optical fibers based on such glasses attract a considerable interest due to a broadband IR luminescence in the range of 1.0 – 1.7 μm employed successfully in fiber lasers and amplifiers (see e.g. the review [8]).

Although the origin of the IR luminescence is still not clear, recently a belief has been strengthened that subvalent bismuth centers are responsible for the luminescence [9]. In our opinion, monovalent bismuth centers are of a particular interest.

Glasses as disordered systems are very complicated to study impurity centers structure. In this regard, crystals may be of interest as model hosts containing bismuth-related centers. In particular, crystalline halides of monovalent metals are convenient hosts for monovalent bismuth centers. These crystals have a simple structure (primitive, $\text{Pm}\bar{3}\text{m}$, or face-centered, $\text{Fm}\bar{3}\text{m}$, cubic lattice). Bismuth can easily form monovalent substitutional centers in such lattice. Similar subvalent thallium and lead centers in $\text{Fm}\bar{3}\text{m}$ crystals were studied extensively (e.g. thallium in KCl [10] and lead in MF_2 , $\text{M} = \text{Ca}, \text{Sr}, \text{Ba}$ [11]). By analogy, the models of bismuth-related centers in oxide glasses for fiber optics were suggested [12].

Bismuth-related IR luminescence in cubic halide crystals was studied for the first time in BaF_2 [13], then in CsI ($\text{Pm}\bar{3}\text{m}$) [2, 3] and recently in TlCl ($\text{Pm}\bar{3}\text{m}$) [1]. Two models of the centers in CsI:Bi were suggested in [2, 3], namely, a monovalent bismuth substitutional center, Bi^+ , and a dimer center, Bi_2^+ , formed by two Bi^+ substitutional centers in the nearest cation sites with an extra electron. In what follows we report the results of com-

puter modeling of bismuth-related centers in TlCl:Bi and CsI:Bi crystals.

II. MODELING OF BISMUTH-RELATED CENTERS IN TlCl:BI AND CsI:BI CRYSTALS

To study the origin of the IR luminescence in TlCl:Bi and CsI:Bi, we performed a computer simulation of the structure and absorption spectra of three bismuth-related centers possibly occurring in both crystals. Basing on the assumptions made in [2, 3] and on analogy with $\text{Tl}^0(1)$ centers in alkaline halide crystals (see e.g. [10]), we studied the Bi^+ substitutional center as the main form of bismuth embedding in TlCl and CsI, the Bi_2^+ dimer center, and $\text{Bi} \cdots \text{V}_{\text{Cl}}$ and $\text{Bi} \cdots \text{V}_{\text{I}}$ complexes formed by the bismuth substitutional center and anion vacancy in its first coordination shell.

The modeling was performed in a supercell approach. $3 \times 3 \times 3$ TlCl or CsI supercells (54 atoms) was chosen to model Bi^+ and $\text{Bi} \cdots \text{V}_{\text{Cl}}$ or $\text{Bi} \cdots \text{V}_{\text{I}}$ centers, and $3 \times 3 \times 4$ supercell (72 atoms) was used for Bi_2^+ . In the central region of the supercell certain cations were substituted by bismuth atoms and an anion vacancy was formed by a removal of one chlorine or iodine atom. Charged centers were simulated changing the total number of electrons in the supercell. Equilibrium configurations of bismuth centers were found by a complete optimization of the supercell parameters and atomic positions with the gradient method. All such calculations were performed using Quantum-Espresso package [14] in the plane wave basis in the generalized gradient approximation of density functional theory with ultra-soft pseudopotentials built with PBE functional [15]. The pseudopotential sources were taken from the pslibrary v. 0.3.0 pseudopotential library [16].

To test the approach, TlCl and CsI lattice parameters were calculated for the unit cell and supercells with both atomic positions and cell parameters completely optimized. The results convergence was tested with respect to the plane wave cutoff energy and to the k points grid.

* E-mail: vence.s@gmail.com

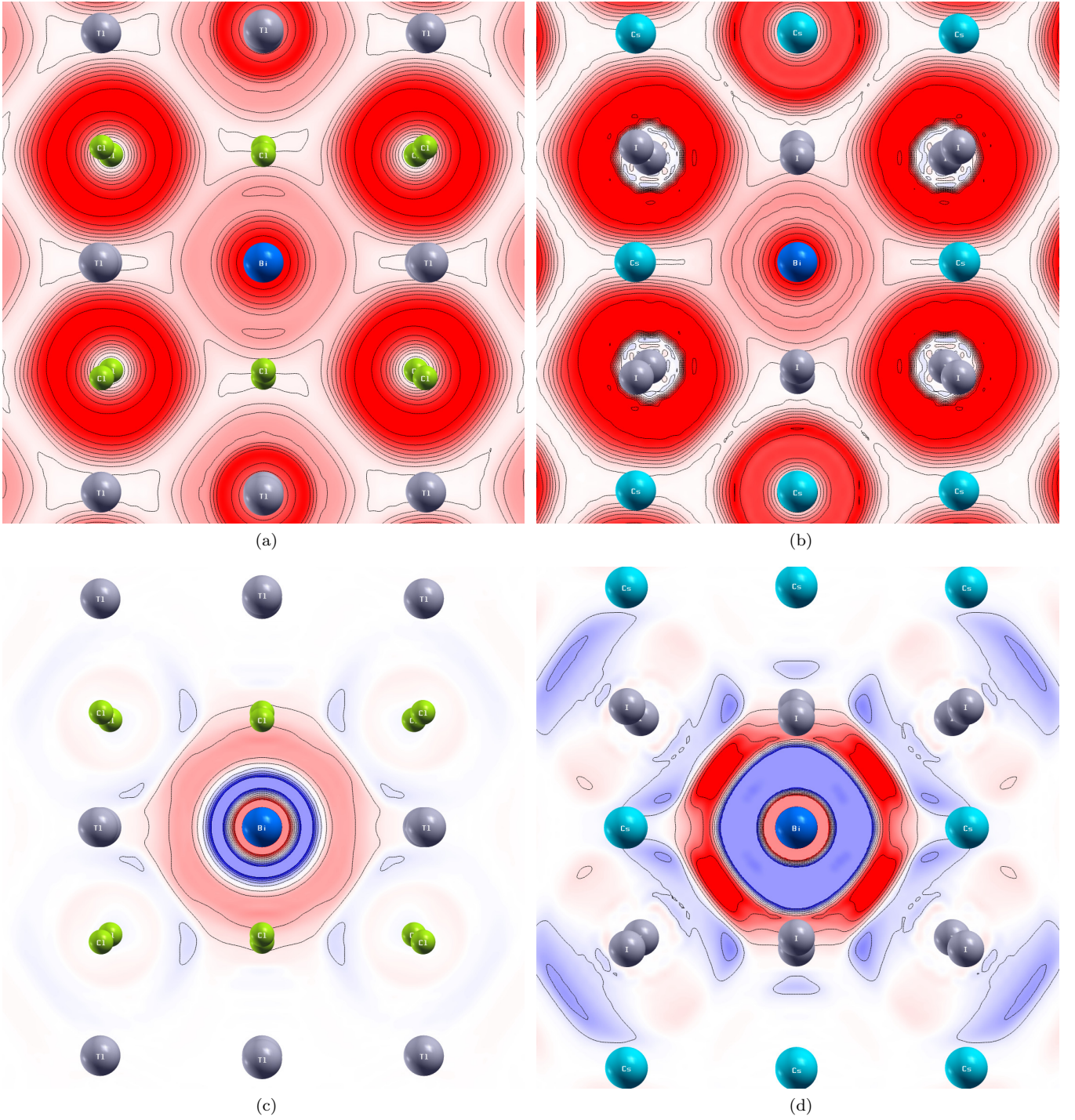


Figure 1. Calculated electron localization functions of Bi^+ substitutional centers in (a) TlCl and (b) CsI , and difference of calculated electron localization functions of Bi^+ center from those of perfect lattice: (a) $\text{TlCl}:\text{Bi}$, (b) $\text{CsI}:\text{Bi}$ (in the (111) plane).

The energy cutoff $\gtrsim 700$ eV and the number of k points ≥ 27 in the irreducible part of the unit cell Brillouin zone were found to be enough to converge the total energy within 10^{-3} eV per atom and to reproduce the experimental lattice parameters with a relative accuracy of $\lesssim 1\%$. The geometry of each supercell was reproduced

with a relative accuracy better than 2% with only Γ point of the supercell taken into account and better than 1% using 8 k points in the supercell in the irreducible part of the supercell Brillouin zone. The total energy convergence was not worse than that in the case of the unit cell.

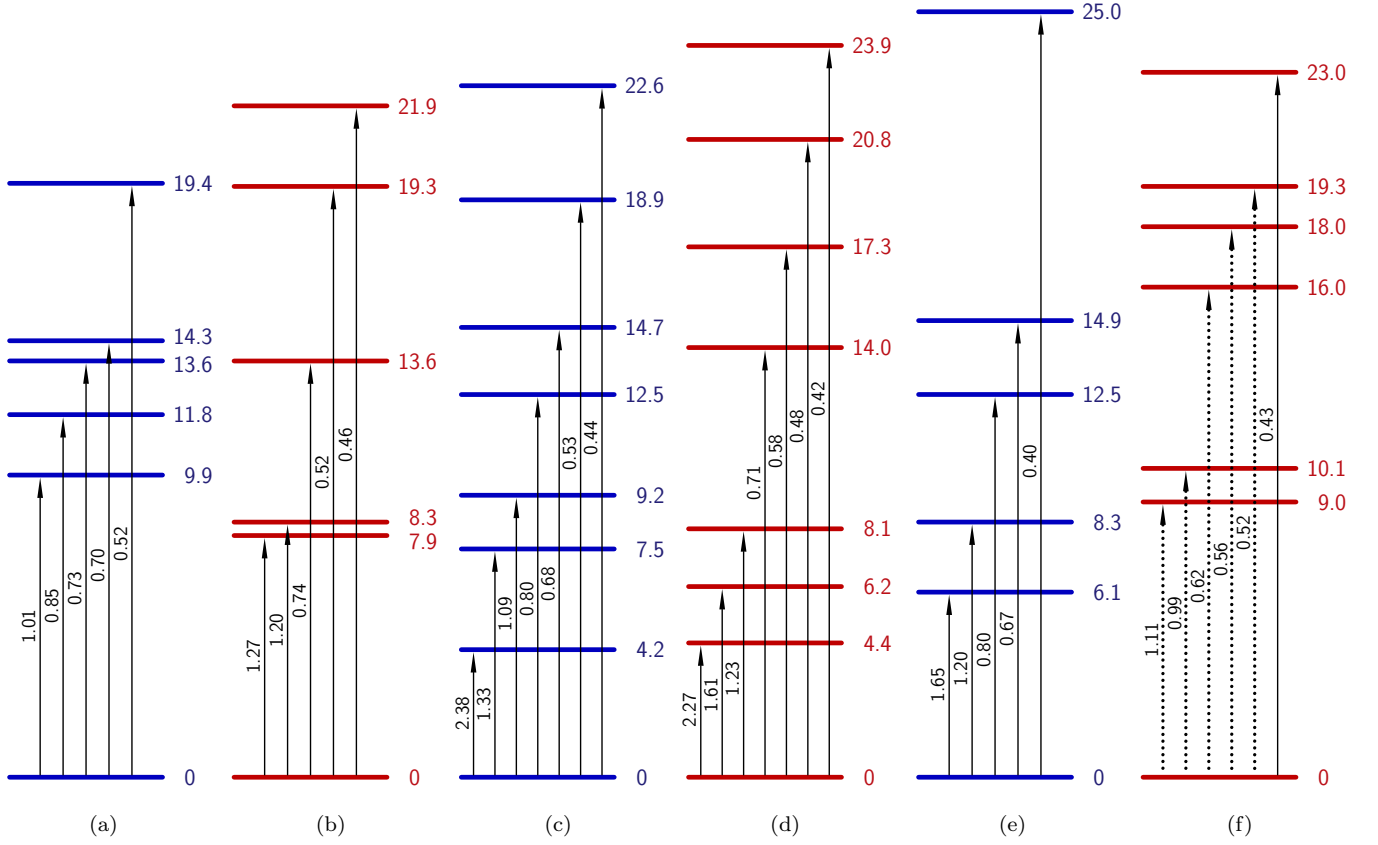


Figure 2. Calculated level and transition schemes of bismuth-related centers: (a) Bi^+ substitutional center in $\text{TlCl}:\text{Bi}$, (b) Bi^+ substitutional center in $\text{CsI}:\text{Bi}$, (c) Bi_2^+ dimer center in $\text{TlCl}:\text{Bi}$, (d) Bi_2^+ dimer center in $\text{CsI}:\text{Bi}$, (e) $\text{Bi}^+ \cdots \text{V}_{\text{Cl}}^-$ center in $\text{TlCl}:\text{Bi}$, (f) $\text{Bi}^0 \cdots \text{V}_{\text{I}}^0$ center in $\text{CsI}:\text{Bi}$. Level energies are given in 10^3 cm^{-1} , transition wavelengths in μm .

Configurations of bismuth-related centers obtained by this means were used to calculate the electron localization functions using the programs from Quantum-Espresso package, the electron density distribution and effective charges of atoms by Bader's method using bader v. 0.28 code [17], and the absorption spectra of the centers by Bethe-Salpeter equation method based on all-electron full-potential linearized augmented-plane wave approach [18]. The absorption spectra calculations were performed using Elk code [19] in the local spin density approximation with PW-CA functional [20, 21]. Spin-orbit interaction essential for bismuth-containing systems was taken into account. Scissor correction was applied to transition energies calculation with the scissor value found using modified Becke-Johnson exchange-correlation potential known to yield accurate band gaps in many solids [22–24]. The non-overlapping muffin-tin (MT) spheres of maximal possible radii $R_{\text{MT}}^{\text{MT}}$ were used. Convergence of the results was tested with respect to plane-wave cutoff energy, to the angular momentum cutoff for the MT density and potential, and to the k points grid choice. The plane-wave cutoff, k_{max} , was determined by the $R_{\text{min}}^{\text{MT}} \cdot k_{\text{max}} = 7$ relation with $R_{\text{min}}^{\text{MT}}$ being the smallest MT radius. The angular momentum cut-off was taken to be $l = 10$. The

self-consistent calculations were performed on the $3 \times 3 \times 3$ grid of k points uniformly distributed in the irreducible part of the supercell Brillouin zone. Further increasing the cutoff and k points density did not lead to significant changes in the results. The total energy self-consistence tolerance was taken to be 10^{-3} eV per atom. More dense $4 \times 4 \times 4$ k points grid was applied to calculate dipole matrix elements in optical spectra calculations.

Simplified configurational coordinate diagrams of bismuth-related centers were calculated in a model restricted to the lowest excited states with a displacement of bismuth atom(s) along [111] axis for Bi^+ and $\text{Bi}^0 \cdots \text{V}_{\text{I}}^0$ centers and along [001] axis for Bi_2^+ center. In spite of the fact that the model is inherently rough, it shows that in all the centers studied the Stokes shift corresponding to a transition from the first excited state to the ground one do not exceed the accuracy of the excited state energy calculation. Hence it seems reasonable enough to estimate the IR luminescence wavelengths by taking this Stokes shift to be zero.

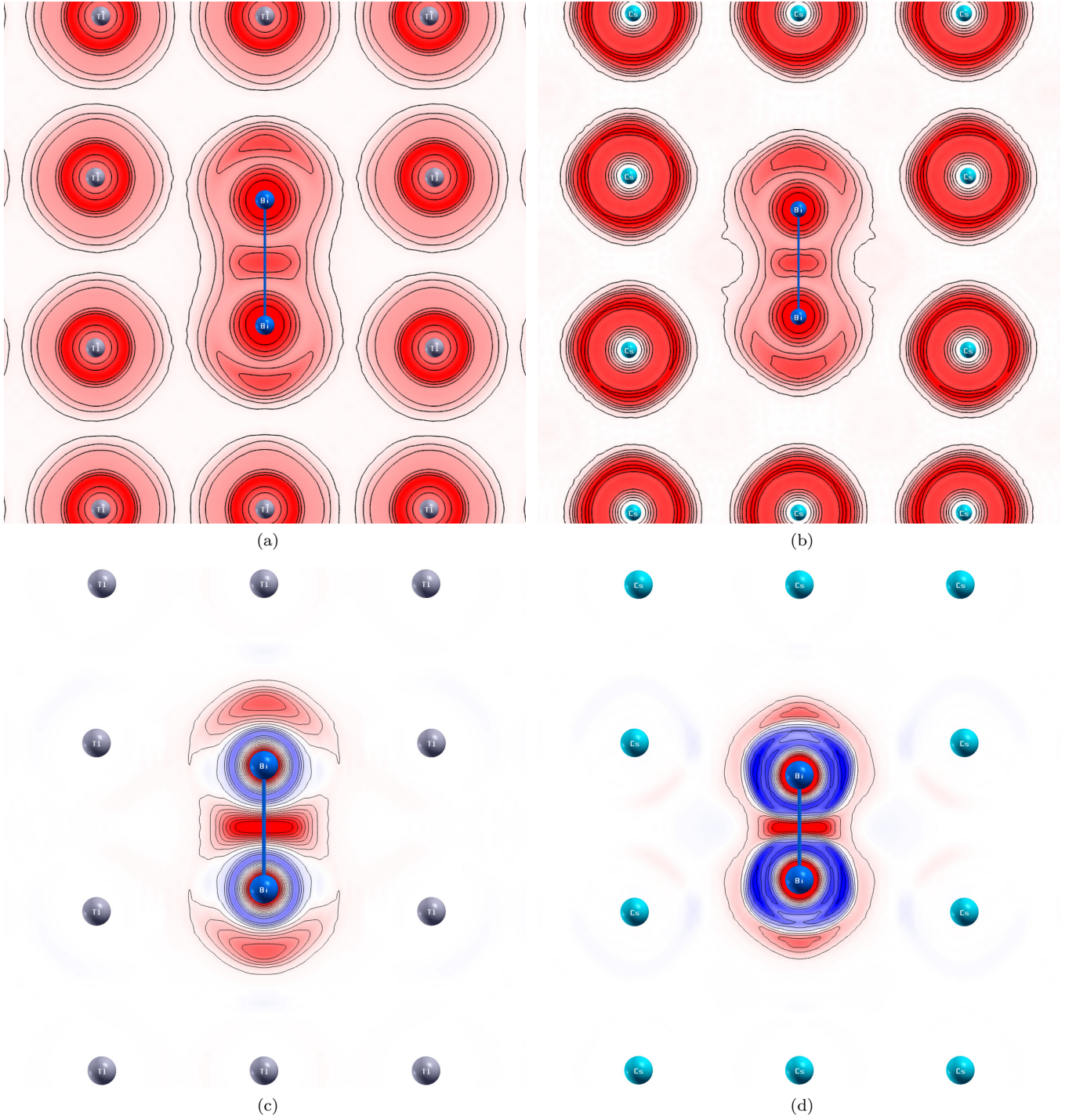


Figure 3. Calculated electron localization functions of Bi_2^{+} dimer centers in (a) TlCl and (b) CsI, and difference of calculated electron localization functions of Bi_2^{+} dimer center from those of perfect lattice: (c) TlCl:Bi, (d) CsI:Bi (in the (101) plane).

III. RESULTS AND DISCUSSION

A. Bi^{+} substitutional centers

Calculation of Bi^{+} substitutional center shows that both in TlCl and in CsI the crystal lattice is distorted

rather slightly around it: bismuth atom lies in the cation site, the nearest chlorine or iodine atoms are displaced by almost $0.1a$ towards the bismuth cite, a being the crystal lattice constant ($a \approx 0.3834$ nm in TlCl and $a \approx 0.4565$ nm in CsI), and the nearest thallium or cesium atoms are displaced apart from the bismuth cite. So

Bi–Cl and Bi–Tl distances are 0.3120 and 0.3889 nm, respectively (0.3320 and 0.3834 nm in perfect TlCl crystal) and Bi–I and Bi–Cs distances are 0.3641 and 0.4624 nm, respectively (0.3955 and 0.4567 nm in perfect CsI crystal).

Bader analysis of the electron density around Bi^+ center in TlCl showed the atomic effective charges to be $+1.03|e|$, $-0.70|e|$, and $+0.73|e|$ in bismuth atom, in each of the nearest chlorine atoms, and in each of the nearest thallium atoms, respectively. The same analysis in CsI yielded $+0.75|e|$, $-0.67|e|$, and $+0.80|e|$ atomic effective charges in bismuth atom, in each of the nearest iodine atoms, and in each of the nearest cesium atoms, respectively. The effective atomic charges in perfect TlCl and CsI crystal lattices calculated by the same approach were found to be $-0.73|e|$ and $+0.73|e|$ in chlorine and thallium atoms, respectively, and $-0.80|e|$ and $+0.80|e|$ in iodine and cesium atoms, respectively.

In TlCl the total charge localized in cation site and the neighboring anion sites was changed from $-3.65|e|$ in perfect lattice to $-3.17|e|$ in the lattice with bismuth substitutional center. In CsI this total charge was changed from $-4.00|e|$ in perfect lattice to $-3.27|e|$ in the lattice with bismuth substitutional center. This shows that the electron density was displaced into the space between bismuth atom and the nearest anions and may be considered as slight covalent contribution to Bi–Cl and Bi–I interaction. In CsI such displacement is more noticeable (Fig. 1).

The calculated energy levels of the Bi^+ center in TlCl:Bi and CsI:Bi are shown in Figs. 2(a) and 2(b), respectively, together with the corresponding transitions. It should be noticed that splitting of the Bi^+ ion states in bismuth substitutional centers in TlCl:Bi and CsI:Bi is not described by crystal field theory due to total cubic symmetry of bismuth ion environment, unlike to the case of $\text{Tl}^0(1)$ center [10]. In this case the splitting is caused by electron density redistribution with a covalent contribution formed. Absorption near 1.0, 0.8, 0.7, and $\sim 0.5 \mu\text{m}$ is found in the Bi^+ center in TlCl. The above-mentioned excited states evaluative calculation allows one to expect a luminescence in TlCl:Bi near $1.0 \mu\text{m}$ excited in this absorption bands. In CsI:Bi the IR luminescence in the $1.2\text{--}1.3 \mu\text{m}$ range may be expected to be excited in absorption bands near 1.2, 0.7, 0.5, and $\gtrsim 0.45 \mu\text{m}$. Besides, in TlCl:Bi another one luminescence transition, with much a lower lifetime, may occur near $0.8 \mu\text{m}$.

B. Bi_2^+ dimer centers

The modeling shows that the Bi_2^+ dimer centers can actually occur both in CsI and TlCl crystals.

In Bi_2^+ centers the bismuth atoms are found to be displaced from the adjacent cation sites by $0.12a$ and $0.18a$ towards each other, so that the Bi–Bi distance is reduced to 0.2903 and 0.2961 nm in TlCl:Bi and CsI:Bi,

respectively. The nearest chlorine or iodine atoms are displaced towards the dimer, and the nearest thallium or cesium atoms are displaced apart from the dimer. As a result, the Bi–Cl and Bi–Tl distances are 0.3060 and 0.3960 nm, respectively (0.3320 and 0.3834 nm, respectively, in perfect TlCl crystal), and the Bi–I, and Bi–Cs distances become 0.3314 and 0.4743 nm, respectively, as compared to 0.3955 and 0.4567 nm, respectively, in perfect CsI lattice.

Bader’s method analysis of electron density around the center shows that the excess electron charge, $-1|e|$, is localized almost completely in the first coordination shell of two bismuth sites, mainly in bismuth atoms and partially in the nearest chlorine or iodine atoms (Fig. 3). In TlCl:Bi the effective charge in each of the bismuth atoms is found to be $+0.82|e|$, and the effective charge in each of the nearest chlorine and thallium atoms is $-0.73|e|$ and $+0.72|e|$, respectively. So, as compared to Bi^+ center, positive charge in each of the bismuth atoms is decreased by $0.21|e|$, negative charge in each of the neighboring chlorine atoms is increased by $0.03|e|$, and positive charge in each of the nearest thallium atoms is decreased by $0.01|e|$. Hence the excess total charge localized in two bismuth atoms and their nearest neighbors turns out to be $\approx -0.6|e|$. In CsI:Bi the effective charge in each of the bismuth atoms is $+0.48|e|$, and the effective charge in each of the nearest iodine and cesium atoms is $-0.70|e|$ and $+0.79|e|$, respectively. As compared to Bi^+ center, positive charge in each of the bismuth atoms is decreased by $0.27|e|$, negative charge in each of the neighboring iodine atoms is increased by $0.03|e|$, and positive charge in each of the nearest cesium atoms is decreased by $0.01|e|$. So the excess total charge in two bismuth atoms and their environment is $\approx -0.7|e|$. So the center is actually Bi_2^+ dimer both in TlCl:Bi and in CsI:Bi. However, again a certain part of the electron density is displaced into the space between bismuth atoms and the nearest anions, as in Bi^+ centers.

The calculated energy levels of Bi_2^+ center in TlCl and CsI and the corresponding transitions are shown in Figs. 2(c) and 2(d), respectively. Basing on the evaluative calculations of the first excited state one might expect the IR luminescence bands in TlCl:Bi near 1.1 and $1.3 \mu\text{m}$ excited in absorption near 1.1, 0.8, 0.7, 0.5 and $\sim 0.4 \mu\text{m}$, and in CsI:Bi near 1.2 and $1.6 \mu\text{m}$ excited in absorption near 1.2, 0.7, 0.6, and $\lesssim 0.5 \mu\text{m}$. One more luminescence band near $\sim 2.4 \mu\text{m}$ in TlCl:Bi and in the $\gtrsim 2.2 \mu\text{m}$ range in CsI:Bi corresponding to a transition from the lowest excited state might be observable at a low temperature.

C. Bi substitutional – anion vacancy complex centers

The modeling of the $\text{Bi} \cdots V_{\text{anion}}$ complexes shows that the complexes in TlCl and CsI differ significantly in electronic and spectral properties. The $\text{Bi} \cdots V_{\text{Cl}}$ complex

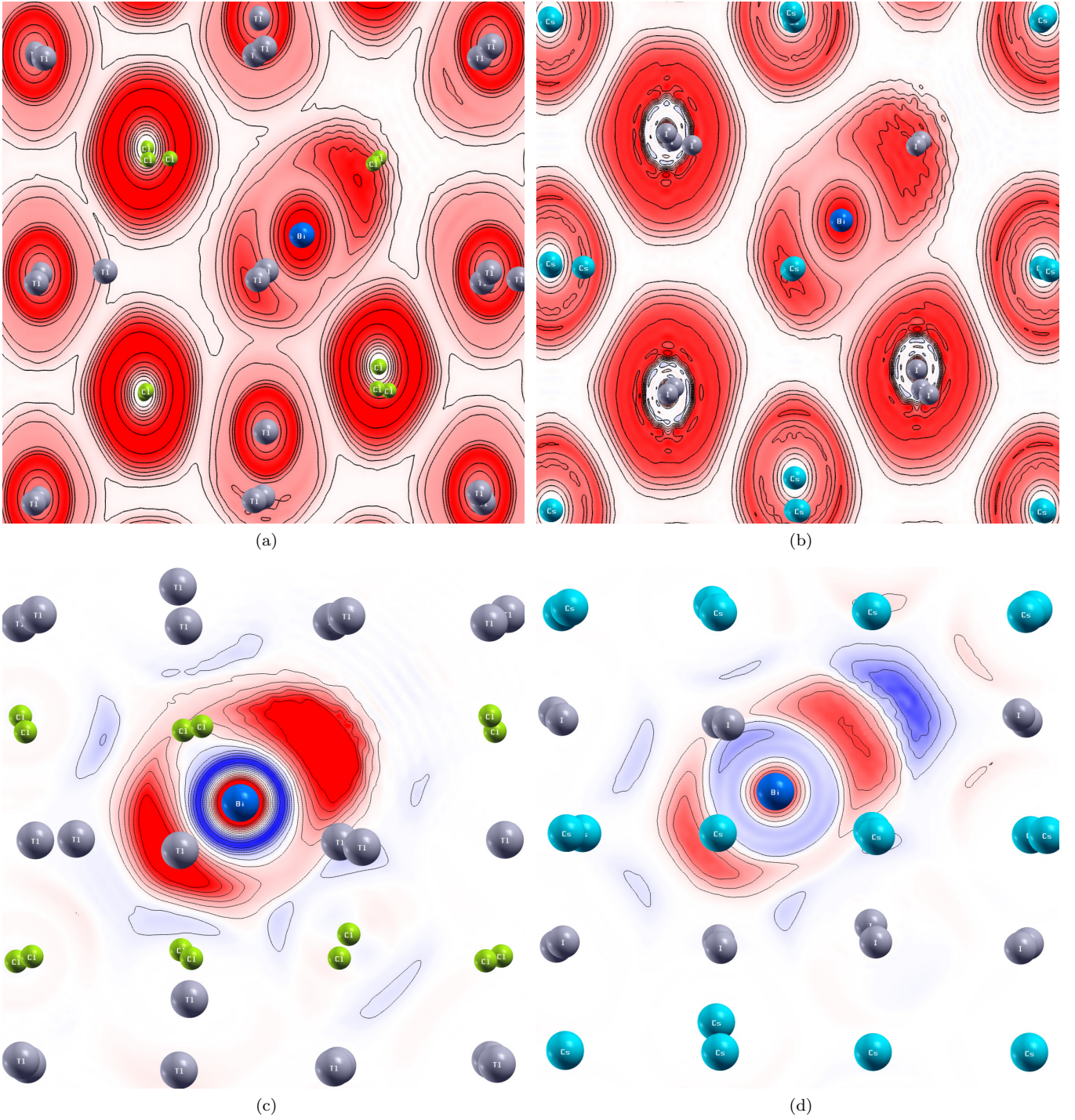


Figure 4. Calculated electron localization functions of (a) $\text{Bi}^+ \cdots \text{V}_{\text{Cl}}^-$ center in $\text{TlCl}:\text{Bi}$ and (b) $\text{Bi}^0 \cdots \text{V}_{\text{I}}^0$ center in $\text{CsI}:\text{Bi}$ (in the (100) plane) and difference of calculated electron localization functions of (a) $\text{Bi}^+ \cdots \text{V}_{\text{Cl}}^-$ center in $\text{TlCl}:\text{Bi}$ from those of perfect crystal and (b) $\text{Bi}^0 \cdots \text{V}_{\text{I}}^0$ center in $\text{CsI}:\text{Bi}$ from those of perfect crystal (in the (111) plane).

in $\text{TlCl}:\text{Bi}$ turns out to be similar in certain respect to $\text{Tl}^0(1)$ centers in alkali halide crystals. However, the $\text{Bi} \cdots \text{V}_{\text{I}}$ complex in CsI differs strikingly from both the $\text{Bi} \cdots \text{V}_{\text{Cl}}$ and $\text{Tl}^0(1)$ centers.

In the $\text{Bi} \cdots \text{V}_{\text{Cl}}$ complex in TlCl the lattice relaxation

turns out to be significant. The bismuth atom is displaced by $0.30a$ from cation site towards the vacant chlorine site, the nearest chlorine and thallium atoms are displaced towards bismuth atom, and thallium atoms surrounding chlorine vacancy are displaced apart from the

vacant site. This results in Bi–Cl, Bi–Tl, and Tl–V_{Cl} distances being 0.3024, 0.3598, and 0.4009 nm, respectively, as compared to the distances 0.3320, 0.3834, and 0.3320 nm in perfect TlCl crystal. The relaxation is accompanied by the electron density shifted from bismuth atom into the chlorine vacancy region, so that the complex center may be thought of as a bound pair of ions, “Bi⁺ plus negatively charged V_{Cl}[−] vacancy” (Fig. 4(a)). Thus this center is a Bi⁺ ⋯ V_{Cl}[−] complex.

In Bi ⋯ V_I complex in CsI, on the one hand, the lattice relaxation is as significant as that in Bi⁺ ⋯ V_{Cl}[−] center. Bismuth atom is displaced by 0.18*a* from the cation site towards the vacant iodine site, the nearest iodine atoms are displaced towards bismuth atom, but the nearest cesium atoms are displaced apart from bismuth atom. This results in Bi–Cs and Bi–I distances decreased to 0.4220 and 0.3509 nm, respectively, from 0.4567 and 0.3955 nm, respectively, in perfect CsI crystal. On the other hand, the electron density distribution turns out to differ strikingly from that in Bi⁺ ⋯ V_{Cl}[−] complex in TlCl crystal. As distinct from TlCl, the electron density in CsI is not redistributed between bismuth atom and anion vacancy. So the Bi ⋯ V_I complex may be roughly thought of as a bound pair: a neutral substitutional atom, Bi⁰, and a neutral iodine vacancy, V_I⁰ (Fig. 4(b)). In other words, this center turns out to be a Bi⁰ ⋯ V_I⁰ complex.

Bader’s method analysis of the electron density distribution around the center confirms these conclusions. In TlCl the effective charge of bismuth atom is +0.79 |e|, effective charge of each of the nearest chlorine atoms is −0.70 |e|, and effective charge of each of the thallium atoms surrounding the chlorine vacancy is +0.66 |e|. So the excess (in comparison with perfect TlCl lattice) positive charge localized in bismuth substitutional atom and its nearest neighbors is about 0.85 |e|, and the negative charge no less than 0.4 |e| is localized in the chlorine vacancy and in its nearest neighbors. In CsI the effective charge of bismuth atom is −0.02 |e|, effective charge of each of the nearest iodine atoms is −0.82 |e|, and effective charge of each of the cesium atoms surrounding the iodine vacancy is +0.79 |e|. So the bismuth substitutional atom turns out to be practically a neutral atom, the excess (in comparison with perfect CsI lattice) positive charge localized in its nearest neighbors is about 0.08 |e| and the positive charge no less than 0.06 |e| is localized in the iodine vacancy and in its nearest neighbors.

The calculated energy levels of Bi⁺ ⋯ V_{Cl}[−] and Bi⁰ ⋯ V_I⁰ centers and the corresponding transitions are shown in Figs. 2(e) and 2(f), respectively. Spectral properties of the Bi⁺ ⋯ V_{Cl}[−] and Bi⁰ ⋯ V_I⁰ complexes may be understood in a model similar to Tl⁰(1) center theory [10]. In such a model the complexes are considered as Bi⁺ ion or Bi⁰ atom, respectively, in the axial crystal field formed by neighboring chlorine or iodine vacancy. Obviously, the crystal field of a negatively charged chlorine vacancy is stronger than that of a neutral iodine vacancy.

Three lowest states of Bi⁺ ion are known to arise from

³P atomic state split by strong spin-orbital interaction in bismuth. The ground state of Bi⁺ ion is ³P₀. The first excited state, ³P₁, is split by an axial crystal field in two levels, 6100 and 8300 cm^{−1}, and the second excited state, ³P₂, is split in three levels, 12500, 14900 and 25000 cm^{−1}. In a free Bi⁺ ion the electric dipole (E1) transitions between three spin-orbital components of the ³P state are forbidden but under the influence of the crystal field the transitions become allowed. Basing on the above-mentioned evaluative calculations one expects the IR luminescence in two bands near 1.6 and 1.2 μm, both excited in absorption near 0.8, 0.7, and ~ 0.4 μm. A luminescence band with a significantly shorter (by an order of magnitude) lifetime may occur near 0.8 μm.

The ground state of Bi⁰ atom is known to be ⁴S_{3/2}. The first excited state, ²D_{3/2}, is split by an axial crystal field in two levels, 9000 and 10100 cm^{−1}. The second excited state, ²D_{5/2}, is split in three levels, 16000, 18000, and 19300 cm^{−1}, and the forth excited state, ²P_{1/2}, is not split by an electrostatic field. Notice that the splitting is expected to be considerably slighter than that in Bi⁺ ⋯ V_{Cl}[−] complex. E1 transitions from the ground state of Bi⁰ ⋯ V_I⁰ center, corresponding to the ⁴S_{3/2} atomic state, to all the states arising from the ²D one, turn out to be weak since in a free atom such transitions are parity-forbidden. Hence the only relatively intensive absorption band near 0.43 μm corresponding to ⁴S_{3/2} → ²P_{1/2} transition may be expected to occur in the Bi⁰ ⋯ V_I⁰ center (Fig. 2(f)). With the above-mentioned evaluative calculations taken into account one might expect that 1.0 – 1.1 μm luminescence corresponding to ²D_{3/2} → ⁴S_{3/2} transitions is excited in this absorption band.

IV. CONCLUSIONS

Spectroscopic data [1–3] and the present results of modeling of bismuth-related centers in TlCl:Bi and CsI:Bi crystals suggest that different centers are responsible for the near-infrared luminescence in these crystals.

In TlCl:Bi the luminescence observed near 1.2 μm is caused mainly by Bi ⋯ V_{Cl} complexes formed by Bi⁺ substitutional ions and negatively charged chlorine vacancies. However, the bismuth-related contribution to the total absorption is caused mainly by single Bi⁺ substitutional centers not contributing to the IR luminescence. This explains a significant difference between the IR luminescence excitation spectrum and TlCl:Bi absorption spectra [1]. Bi⁺ substitutional centers may cause a luminescence near 1.0 μm not observed in [1].

In CsI:Bi the IR luminescence is caused mainly by two types of bismuth centers: Bi⁺ substitutional centers give rise to a luminescence observed in the 1.2 – 1.3 μm range, and Bi₂⁺ dimer centers cause a luminescence observed near 1.2 μm and near 1.6 μm. These conclusions agree with the experimental data of [2, 3] and confirm the as-

sumptions made there. Besides, dimer centers may cause possible luminescence in the $\gtrsim 2.2 \mu\text{m}$ range not observed in Refs. [2, 3].

Bi_2^+ dimer complexes in TlCl:Bi can contribute perceptibly neither to the IR luminescence spectra nor to the absorption spectra, as distinct from CsI:Bi crystals.

$\text{Bi} \cdots \text{V}_\text{I}$ complexes formed in CsI:Bi by Bi^0 substitutional atoms and neutral iodine vacancies may contribute to the IR luminescence only near $1.0 \mu\text{m}$, as distinct from TlCl:Bi crystals. One might suppose that the luminescence in the $0.95 - 1.15 \mu\text{m}$ range observed in [2] at a low temperature under $0.4 - 0.5 \mu\text{m}$ excitation is contributed

by $\text{Bi}^0 \cdots \text{V}_\text{I}^0$ centers formed due to electrons capturing in Bi^+ substitutional centers in the vicinity of iodine vacancies.

ACKNOWLEDGMENTS

This work is supported in part by Fundamental Research Program of the Presidium of the Russian Academy of Sciences and by Russian Foundation for Basic Research (grant 12-02-00907).

-
- [1] V. G. Plotnichenko, V. O. Sokolov, D. V. Philippovskiy, I. S. Lisitsky, M. S. Kouznetsov, K. S. Zaramenskikh, and E. M. Dianov, *Opt. Lett.* **38**, 362 (2013).
 - [2] L. Su, H. Zhao, H. Li, L. Zheng, G. Ren, J. Xu, W. Ryba-Romanowski, R. Lisiecki, and P. Solarz, *Opt. Lett.* **36**, 4551 (2011).
 - [3] L. Su, H. Zhao, H. Li, L. Zheng, X. Fan, X. Jiang, H. Tang, G. Ren, J. Xu, W. Ryba-Romanowski, R. Lisiecki, and P. Solarz, *Opt. Materials Express* **2**, 757 (2012).
 - [4] G. Blasse and A. Bril, *J. Chem. Phys.* **48**, 217 (1968).
 - [5] M. J. Weber and R. R. Monchamp, *J. Appl. Phys.* **44**, 5495 (1973).
 - [6] Y. Fujimoto and M. Nakatsuka, *Japan. J. Appl. Phys.* **40**, L279 (2001).
 - [7] Y. Fujimoto and M. Nakatsuka, *Appl. Phys. Lett.* **82**, 3325 (2003).
 - [8] E. M. Dianov, *J. Non-Cryst. Solids* **355**, 1861 (2009).
 - [9] M. Peng, G. Dong, L. Wondraczek, L. Zhang, N. Zhang, and J. Qiu, *J. Non-Cryst. Solids* **357**, 2241 (2011).
 - [10] L. F. Mollenauer, N. D. Vieira, and L. Szeto, *Phys. Rev. B* **27**, 5332 (1983).
 - [11] M. Fockele, F. Lohse, J.-M. Spaeth, and R. H. Bartram, *J. Phys.: Condens. Matter* **1**, 13 (1989).
 - [12] E. M. Dianov, *Quant. Electronics* **40**, 283 (2010).
 - [13] J. Ruan, L. Su, J. Qiu, D. Chen, and J. Xu, *Opt. Express* **17**, 5163 (2009).
 - [14] P. Giannozzi, S. Baroni, N. Bonini, M. Calandra, R. Car, C. Cavazzoni, D. Ceresoli, G. L. Chiarotti, M. Cococcioni, I. Dabo, A. Dal Corso, S. Fabris, G. Fratesi, S. de Gironcoli, R. Gebauer, U. Gerstmann, C. Gougousis, A. Kokalj, M. Lazzeri, L. Martin-Samos, N. Marzari, F. Mauri, R. Mazzarello, S. Paolini, A. Pasquarello, L. Paulatto, C. Sbraccia, S. Scandolo, G. Sclauzero, A. P. Seitsonen, A. Smogunov, P. Umari, and R. M. Wentzcovitch, *J. Phys.: Condens. Matter* **21**, 395502 (2009).
 - [15] J. P. Perdew, K. Burke, and M. Ernzerhof, *Phys. Rev. Lett.* **77**, 3865 (1996).
 - [16] <http://qe-forge.org/projects/pslibrary>
 - [17] <http://theory.cm.utexas.edu/vtsttools/bader>
 - [18] O. K. Andersen, *Phys. Rev. B* **12**, 3060 (1975).
 - [19] <http://elk.sourceforge.net>
 - [20] J. P. Perdew and Y. Wang, *Phys. Rev. B* **45**, 13244 (1992).
 - [21] D. M. Ceperley and B. I. Alder, *Phys. Rev. Lett.* **45**, 566 (1990).
 - [22] A. D. Becke and E. R. Johnson, *J. Chem. Phys.* **124**, 221101 (2006).
 - [23] F. Tran and P. Blaha, *Phys. Rev. Lett.* **102**, 226401 (2009).
 - [24] D. Koller, F. Tran, and P. Blaha, *Phys. Rev. B* **83**, 195134 (2011).